Geoscience Frontiers 13 (2022) 101350

HOSTED BY

Contents lists available at ScienceDirect

Geoscience Frontiers

journal homepage: www.elsevier.com/locate/gsf

Research Paper

Granular titanite from the Roter Kamm crater in Namibia: Product of regional metamorphism, not meteorite impact

Aaron J. Cavosie [a,*], Christopher J. Spencer [b], Noreen Evans [a,c], Kai Rankenburg [c], Robert J. Thomas [d], Paul H. Macey [d]

[a] Space Science and Technology Centre and The Institute for Geoscience Research, School of Earth and Planetary Science, Curtin University, Perth, WA 6102, Australia
[b] Dept. of Geological Sciences and Geological Engineering, Queen's University, Ontario, Canada
[c] John de Laeter Centre, Curtin University, Perth, WA 6102, Australia
[d] Council for Geoscience, Bellville, Western Cape, South Africa

ARTICLE INFO

Article history:
Received 14 July 2021
Revised 20 December 2021
Accepted 13 January 2022
Available online 19 January 2022
Handling Editor: N.M.W. Roberts

Keywords:
Namibia
Roter Kamm
Titanite
EBSD
Geochronology

ABSTRACT

Accessory minerals with so-called granular texture have risen in importance as geochronological tools for U-Pb dating of meteorite impact events. Grain-scale recrystallization, typically triggered by a combination of high-strain deformation and post-impact heating, can create a polycrystalline microstructure consisting of neoblasts that expel radiogenic Pb, which are thus ideal for isotopic dating. While granular domains in zircon and monazite from shocked rocks have been demonstrated to preserve impact ages, few U-Pb dating studies have been conducted on granular microstructures in titanite ($CaTiSiO_5$). Here we report the occurrence of granular-textured titanite from ~2020 Ma granite basement rock exposed in the rim of the 4–5 Ma Roter Kamm impact structure in Namibia. Orientation mapping reveals two microstructurally distinct titanite populations: one consisting of strained/deformed grains, and the other consisting of grains that comprise aggregates of strain-free neoblasts. *In situ* U-Pb geochronology on 37 grains shows that most grains from both titanite populations yield indistinguishable U-Pb dates of *ca.* 1025 Ma, consistent with the observed microstructures forming during the Mesoproterozoic Namaqua Orogeny. Only four grains preserved older age domains, recording *ca.* 1875 Ma Paleoproterozoic metamorphism. Two significant observations emerge: (1) none of the analyzed titanite grains yield the 2020 Ma igneous crystallization age previously established from zircon in the same sample, and (2) no age-resetting was detected that could be attributed to the 4 to 5 Ma Roter Kamm impact event. Despite the similarity of the neoblastic microstructure to minerals from other sites with an established impact provenance, the granular texture and near-complete Pb-loss in titanite from Roter Kamm granite instead records a Paleo- to Mesoproterozoic polymetamorphic history, rather than Miocene age shock-related processes. These results highlight the critical importance of grain-scale context for interpretation of U-Pb data in granular titanite, and the potential for misinterpreting inherited (pre-impact) microstructures as impact-related phenomenon in target rocks with a complex geological history.

1. Introduction

Accessory mineral U-Pb geochronometers are increasingly being exploited for dating impact events. While commonly associated with impact melt rocks or other rocks that have experienced elevated thermal conditions post-impact, granular textured minerals occur in a wide range of crater environments. The combination of grain orientation mapping and *in situ* geochronology for identification and targeted age dating of recrystallized neoblastic (granular) domains has been demonstrated to yield accurate meteorite impact ages for zircon (e.g., Kenny et al., 2017; Hauser et al., 2019; Kenny et al., 2019; Rasmussen et al., 2020), monazite (e.g., Erickson et al., 2017), and baddeleyite (Darling et al., 2016). The presence of granular neoblastic microstructures have been reported in other accessory minerals from impact melt rocks, including apatite (e.g., Kenny et al. 2020; McGregor et al. 2020), however, there have been few descriptions of this texture in titanite. To date, occurrences of granular textured titanite that have been documented by orientation mapping are limited to studies of rocks from the Sudbury (Canada) and Vredefort (South Africa)

* Corresponding author.
E-mail address: aaron.cavosie@curtin.edu.au (A.J. Cavosie).

https://doi.org/10.1016/j.gsf.2022.101350

impact structures Papapavlou et al., 2017, 2018), and the Lac La Moinerie impact structure (Canada) (McGregor et al., 2021). In the case of Sudbury titanite grains, the recrystallized domains yielded U-Pb ages that are younger than the Sudbury impact indicating no relation to impact processes (Papapavlou et al., 2017). At Vredefort, granular titanite domains were shown to be spatially associated with deformation twins, providing a tentative link to formation by impact processes (Papapavlou et al., 2018). In contrast, granular titanite from the Lac La Moinerie impact structure yielded complex U-Pb age spectra; the microstructure was attributed to impact-generated recrystallization, yet the neoblastic domains were only partially age reset (McGregor et al., 2021). Thus, there remains uncertainty as to whether or not granular texture in titanite can be exploited as a reliable hallmark microstructure of meteorite impact processes for dating purposes, including what microstructural characteristics of recrystalized titanite are uniquely produced by impact, and if impact-generated granular titanite can be distinguished from granular titanite occurrences in endogenic tectonic settings.

Here we use electron backscatter diffraction orientation mapping and targeted *in situ* U-Pb geochronology to determine the mechanism of granular titanite formation in Proterozoic granite basement rocks with a polymetamorphic history from the 4 to 5 Ma Roter Kamm impact crater in Namibia. The rationale to investigate granular titanite at Roter Kamm is driven by three site-specific observations: first, most of the Roter Kamm crater is buried by sand, so the location of the studied sample in the crater rim provides an opportunity for discovery of previously unreported shock effects; second, no crystallographic orientation studies of deformation in accessory minerals have been conducted at the Roter Kamm crater; and third, granites exposed in the rim near where the sample was collected are described as containing pseudotachylite veins, which indicates that they may have experienced elevated pressure and/or temperatures relative to samples from elsewhere in the crater. Our study thus investigates the genesis of this unusual microstructure in titanite and its occurrence in rocks that have experienced both regional and impact-related metamorphism.

2. Geology of the Roter Kamm impact crater

The regional geologic setting of the Roter Kamm impact structure has been reviewed previously (e.g., Reimold and Miller, 1989; Reimold et al., 1994). The crater is located ~10 km south of the Aurus Mountains in southern Namibia (Fig. 1A), the geology of which has been described by Thomas et al. (2016). The Aurus Mountains form a tectonic basement inlier within the Neoproterozoic Gariep belt, known as the Sperrgebiet Domain, which forms the oldest component of the Namaqua sector of the Mesoproterozoic (~1 Ga) Namaqua-Natal orogenic belt. It consists of a number of Palaeoproterozoic calc-alkaline granodioritic orthogneisses and granitoid intrusions dated between ~2.02 and 1.9 Ga. The oldest orthogneisses are grouped into the Wasserkuppe Suite and it is one member of this suite, the Roter Kamm Granite, that forms the uplifted rim of the crater. The granite is coarse-grained, pinkish-grey, weakly foliated and composed of quartz, alkali feldspar, subordinate plagioclase and biotite. The Wasserkuppe Suite intruded synchronously with amphibolite facies metamorphism and deformation, considered to be an early phase of the Palaeoproterozoic Orange River orogeny. The suite is intruded by ~1885 Ma granites which are interpreted as equivalents of the Vioolsdrif Suite, exposed to the south in the Richtersveld magmatic arc (Macey et al., 2017). The Sperrgebiet Domain is thus seen as an early phase of Palaeoproterozoic island-arc development at the margins of the Archaean Kaapvaal Craton/ Rehoboth Province. It was cannibalised by the later Richtersveld arc which contains ~2020 Ma detritus and inherited zircon, as do many other Palaeo- and Mesoproterozoic igneous rocks throughout the Mesoproterozoic Namaqua sector.

Both the Sperrgebiet and Richtersveld domains have only a minor Mesoproterozoic (Namaqua) imprint, but the former was intruded at about 1000 Ma, by small plutons and sheets of leucogranite and pegmatite known as the Warmbad Granite (Thomas et al., 2016), especially in outcrops adjacent to (about 10 km distant from) the Roter Kamm crater. All the other Namaqua sector domains to the south and east have (by definition) a very strong tectonothermal imprint and were intruded by voluminous igneous suites between 1.2 and 1.0 Ga (e.g. Cornell et al. 2006; Macey et al., 2018).

The Roter Kamm impact event produced a 2.5 km diameter simple crater (Fig. 1) that currently is nearly entirely covered by sand (Fig. 1B); outcrops are only found in the raised rim. Exposed rocks include predominantly the Roter Kamm granite (Thomas et al., 2016), with very minor amounts of gneiss, felsic pegmatite, amphibolite, quartz veins, and remnants of the overlying supracrustal rocks (Reimold and Miller, 1989; Reimold et al., 1994). The most conspicuous shock metamorphic effects include quartz grains with up to three orientations of planar deformation features (Reimold et al., 1997). The age of the Roter Kamm impact event is constrained by ^{40}Ar-^{39}Ar analysis of impact glass and impact melt rock to have occurred ca. 4 to 5 Myr ago (Koeberl et al., 1993; Hecht et al., 2008).

Of significance to this study is the observation that extensive networks of dark veins have been reported in exposed rim rocks, including the Roter Kamm granite. The veins are typically mm- to cm-wide and resemble impact melt at outcrop scale; petrographic and geochemical studies have described the veins as either pseudotachyite or cataclasite (Reimold and Miller, 1989; Reimold et al., 1994; Degenhardt et al., 1994). In either scenario, recrystallization has been cited to have produced new grain growth, partially obliterating cataclastic textures (e.g., Degenhardt et al., 1994). While some studies discount the veins as representing impact melt based on microscopic observation and isotopic studies (Rajmon et al., 2005), the extent of any post-impact thermal pulse that may have accompanied recrystallization is not well known.

3. Materials and methods

The sample analyzed, RT15-187, is Roter Kamm granite collected from the southern rim of the crater (Thomas et al., 2016). Roter Kamm granite is a peraluminous high silica (up to ~75 wt.% SiO_2) granite (Reimold et al., 1994; Thomas et al., 2016) with a variably developed foliation (Fig. 1C). Previous U-Pb zircon geochronology on sample RT15-187 yielded a single U-Pb age population of 2020 ± 35 Ma (2σ, MSWD = 1.9), which was interpreted as the magmatic crystallization age (Thomas et al., 2016). The sample analyzed did not contain evidence of the macroscopic dark veins described above in Section 2.

Grains of titanite and zircon from sample RT15-187 were mounted in epoxy resin and polished. Grain imaging and electron backscatter diffraction (EBSD) orientation mapping were conducted using a Tescan Mira3 field emission scanning electron microscope (SEM) in the John de Laeter Centre (JdLC) at Curtin University. Determination of U-Pb dates for titanite using laser ablation inductively-coupled plasma mass spectrometry (LAICPMS) was conducted using a Resonetics 193 nm excimer UV laser and an Agilent 8900 triple quadrupole mass spectrometer in the GeoHistory Facility in the JdLC at Curtin University. A full description of analytical methods is presented in the Supplementary Data.

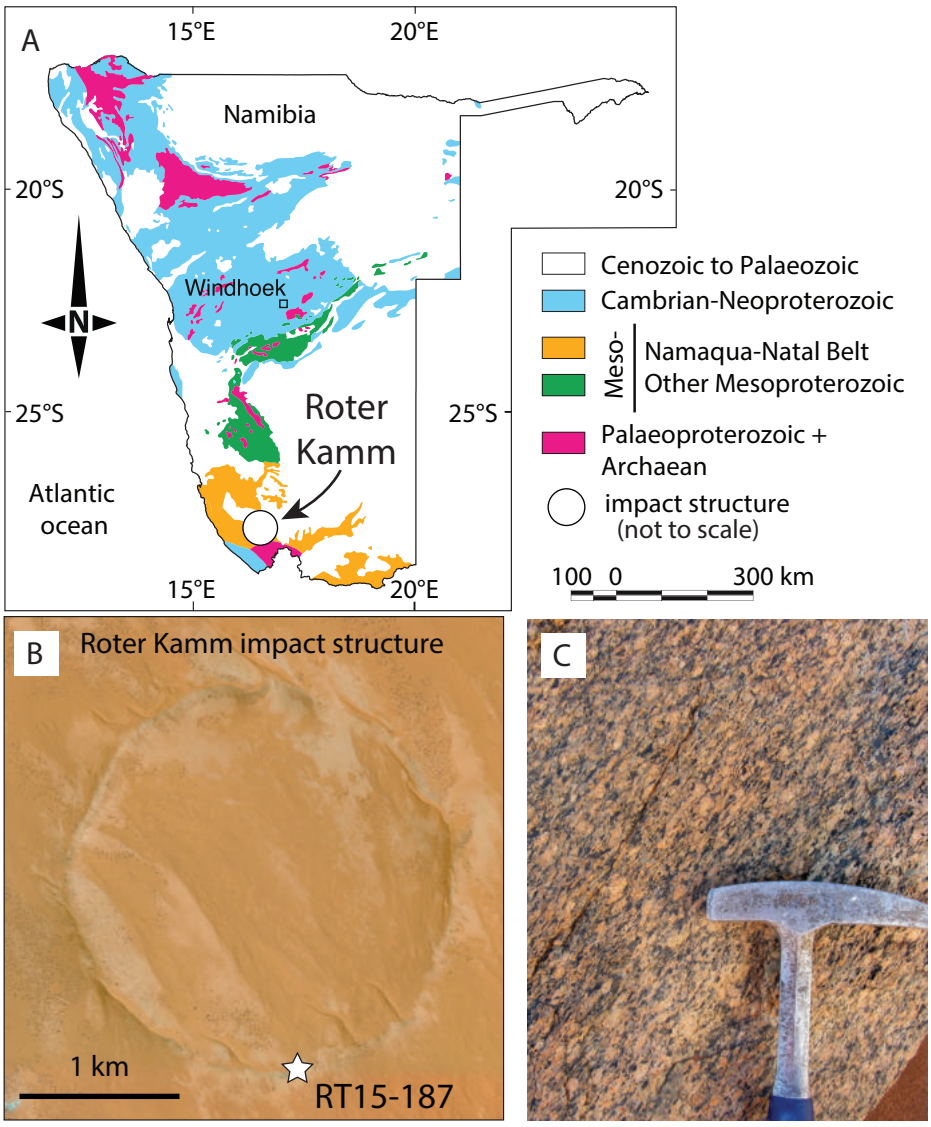

Fig. 1. Features of the Roter Kamm impact structure in southern Namibia. (A) Simplified geological map showing location of the Roter Kamm structure (after Schlüter, 2008). (B) Satellite image of the Roter Kamm impact structure from Google Earth. (C) Photograph of the Roter Kamm granite.

4. Results

4.1. Titanite textures in sample RT15-187

The foliation visible in outcrop (Fig. 1C) manifests in transmitted light images as crude layering defined by quartz, alkali feldspar, and minor remnant plagioclase, interspersed with mafic phases principally consisting of biotite, titanite, clinozoisite, and epidote. Broad domains in thin section are dominated by clinozoisite and epidote (Supplementary Data Figs. S1, S2), and are interpreted as secondary (metamorphic) minerals that formed during alteration of igneous plagioclase. No evidence of shock deformation was observed in the major minerals, such as planar features in quartz, or kink bands in biotite (Supplementary Data Fig. S3), as has been reported in other rocks from the Roter Kamm crater previously (e.g., Reimold et al., 1997).

Petrographic occurrences of titanite include irregularly shaped grains, as well as polycrystalline aggregates (Supplementary Data Fig. S2). Two textural occurrences of titanite were confirmed in BSE images and occur in roughly equal abundance. The first comprises single domain grains with complex internal zoning patterns (Fig. 2A). The second consists of aggregates of neoblastic grains, where conspicuous concentric growth zoning is preserved within individual neoblasts (Fig. 2B, C). Grain orientation mapping using EBSD shows that the population of single-domain grains is variably strained. Some grains appear undeformed, whereas crystal-plastic deformation is present in other grains, preserving up to ~10° of crystallographic misorientation accommodated by low-angle grain boundaries and local development of subgrains. Lamellar deformation twins, dominantly in $\{\bar{1}11\}$ orientation (Timms et al., 2019), are present in some of the non-neoblastic grains (Fig. 2A; Supplementary Data Fig. S4).

The granular titanite grains are nearly strain-free; individual neoblasts preserve <2° of internal crystallographic misorientation, and none are twinned. The neoblasts form triple junctions, and most grain boundaries between adjacent neoblasts are >10° (Supplementary Data Figs S5, S6). Biotite grains intergrown with both titanite populations locally have both straight and cuspate grain boundaries, indicating equilibrium crystallization of both phases. In addition to titanite, orientation mapping of 238 zircon

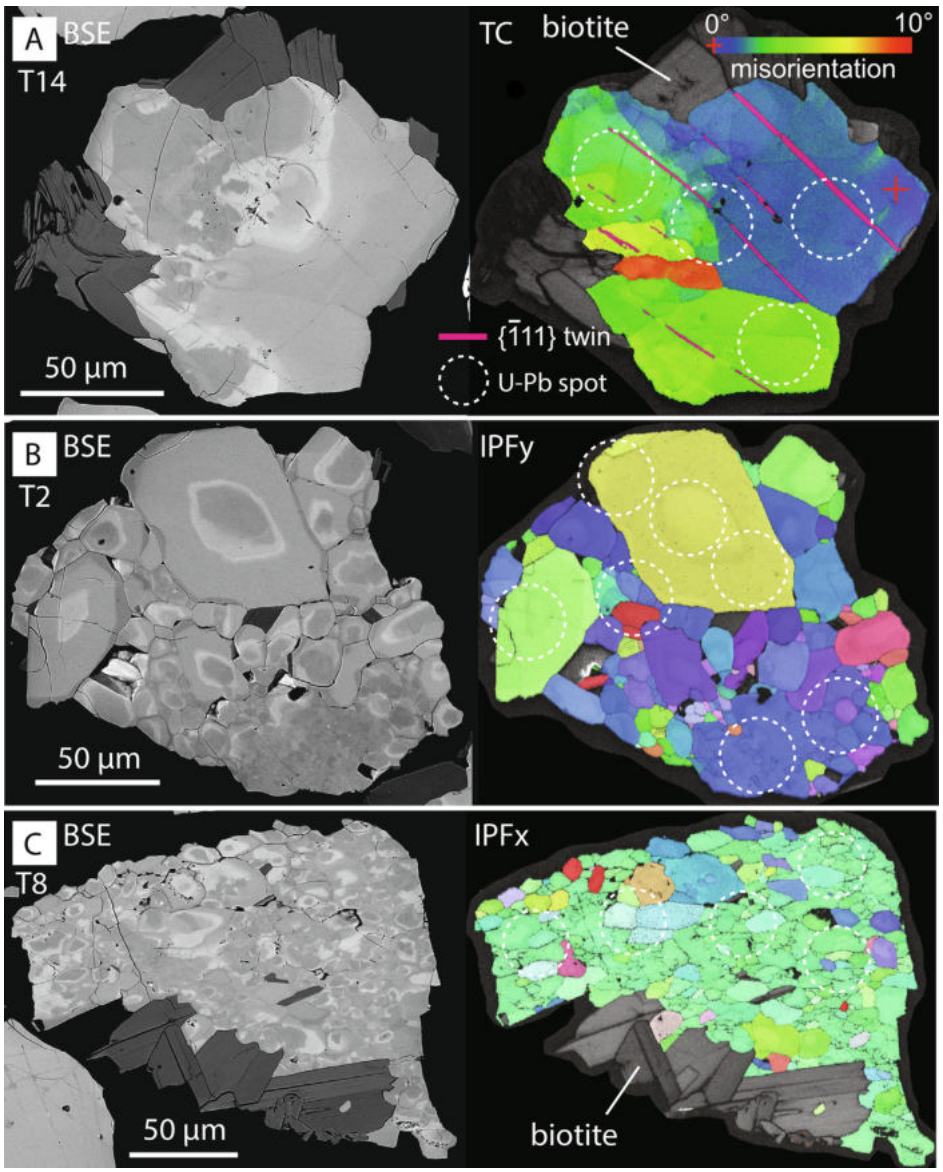

Fig. 2. Examples of titanite textures in Roter Kamm granite. (A) Strained titanite grain, showing disturbed internal zoning (left) and crystal-plastic deformation, and {$\bar{1}$ 11} deformation twins (right). (B) and (C) Examples of granular titanite grains with neoblastic domains. Characteristic features of the neoblasts include concentric zoning (left) and low strain (right). Dashed circles show location of U-Pb age analyses. Pole figures for the grains shown in A, B, C, as well as color legends for B and C, are in the Appendix; pixel size for each orientation map is 250 nm..

grains from sample RT15-187 did not identify any deformation twins, reidite, or evidence of anomalous crystal-plastic deformation (Supplementary Data Fig. S7); no features indicative of shock-deformation were found in zircon.

4.2. Titanite U-Pb data

A total of 307 spot analyses for U-Pb age made on 37 titanite grains (Supplementary Data Table S2) are shown as colored ellipses in Fig. 3 (open ellipses are not included in age regressions). The data were subsequently grouped into spot analyses made in strained grains/domains, and spot analyses made in neoblastic grains/domains. In general, data from both textural domains range from concordant to variably discordant, and broadly define linear arrays; data from strained grains show more complexity compared to data from neoblastic grains (Fig. 3A, B). Data regressions for strained grains (n = 16) and neoblastic grains (n = 12) yield overlapping lower intercept dates of 1032 ± 9 Ma (n = 72, MSWD = 21) and 1047 ± 12 Ma (n = 85, MSWD = 22), respectively (Fig. 3A, B). A minor age component of 1819 ± 75 Ma (n = 4, MSWD = 4) is preserved in some strained grains (Fig. 3A), but was not encountered in neoblastic grains (Fig. 3B). Two additional large grains were chosen for high-density spot analysis (Fig. A8); one yielded a unimodal age population with a lower intercept age of 1014 ± 28 Ma (n = 103, MSWD = 5.9) (Fig. 3C), and the other yielded a bimodal age population, including a dominant younger domain with a lower intercept age of 984 ± 19 Ma (n = 63, MSWD = 6.3) and a minor older age component of 1875 ± 31 Ma (n = 22, MSWD = 0.9) (Fig. 3D). Of the U-Pb analyses from all grains analyzed, 92% (281 of 307) yield Mesoproterozoic ages of *ca.* 1000 Ma, and 8% (26/307) yield Paleoproterozoic ages of *ca.* 1875 Ma. No older or younger age populations than those described above were detected.

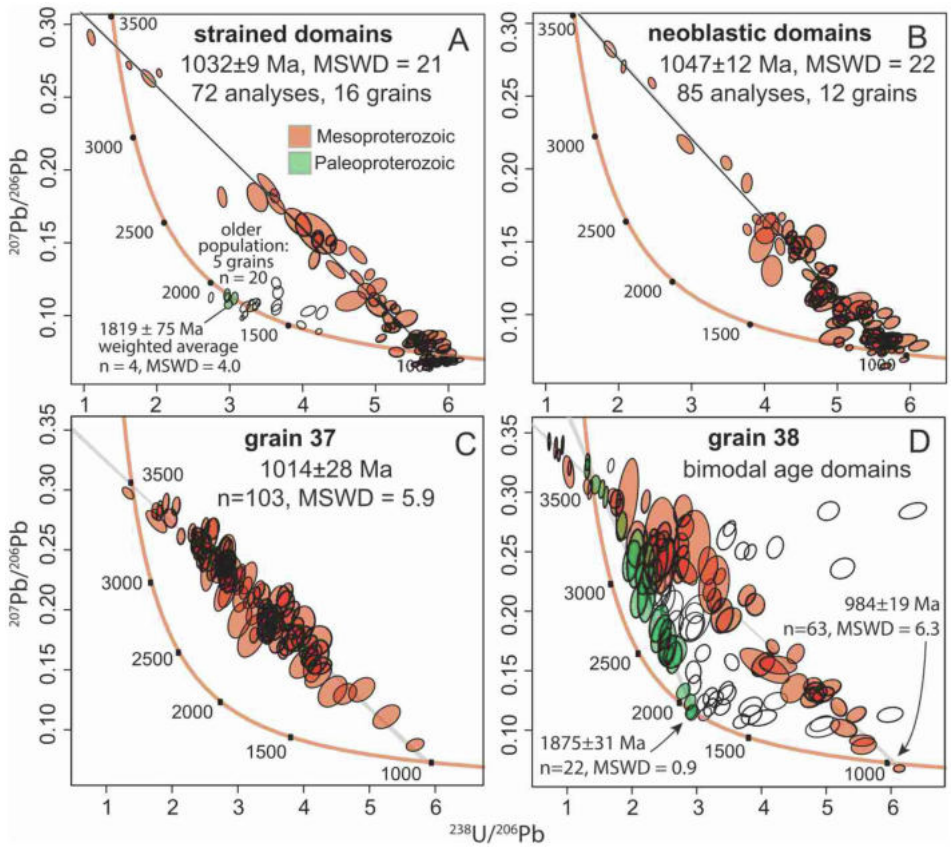

Fig. 3. Results of U-Pb geochronological analysis of titanite. (A) Data for analyses on strained domains; only the red symbols are used for the regression. Note small age population at 1819 ± 75 Ma, colored green. (B) Data for analyses on neoblastic domains, which yielded a single age population (all data included). (C) Data for grain 37, a large grain with a single age population (all data included). (D) Data for grain 38, a large grain with two age populations (colored red and green). The color legend in A applies to all panels.

5. Discussion

5.1. Occurrences of granular titanite at impact settings

We are aware of three previously reported localities where granular titanite is spatially associated with impact structures. Two occurrences of granular titanite (Papapavlou et al., 2017, 2018) were reported from the 1850 Ma Sudbury impact structure in Ontario, Canada (Krogh et al., 1984), which is ~250 km in diameter (Grieve and Therriault, 2000), and thus much larger than Roter Kamm. In both cases, U-Pb dating demonstrated that the Sudbury granular textured titanite formed as a result of processes that significantly post-date the impact event. In the first case, granular titanite in mylonitic rocks from the South Range shear zone comprise elongate aggregates of neoblasts aligned in the foliation; U-Pb ages indicate formation during *ca.* 1700 Ma tectonic deformation, ~150 Myr after the impact (Papapavlou et al., 2017). In the second case, localized neoblasts in partially granular titanite from a South Range pseudotachylite occur near the boundaries of lamellar twins; a single U-Pb age of recrystallized titanite yielded a *ca.* 1700 Ma age (Papapavlou et al., 2018), again much younger than the Sudbury impact event. Granular titanite, at microscopic scale, was also documented at the ~300 km diameter Vredefort dome impact structure in South Africa (Papapavlou et al., 2018). In this case, recrystallization to granular texture was again mostly localized along deformation twin lamellae, with recrystallization interpreted to have occurred during post-impact heating; however, U-Pb analyses made near the Vredefort neoblastic titanite domains yielded only pre-impact Archean bedrock ages (Papapavlou et al., 2018), thus no impact age-resetting was detected.

At the 8 km diameter Lac La Moinerie impact structure in Québec, Canada, granular titanite occurs as mineral clasts within the melt-dominated matrix of impact melt-bearing breccia (McGregor et al., 2021). Recrystallized titanite neoblasts from Lac La Moinerie occur as neoblastic domains that are intergrown with the original host titanite grain; some adjacent neoblasts locally preserve systematic {1 1 1} twin orientation relations, indicating they likely nucleated on or along the {1 1 1} deformation twins. The above observations, along with its occurrence in impact melt, strongly link recrystallization of titanite to elevated pressure and/or temperature conditions produced during impact (McGregor et al., 2021). Two secondary ion mass spectrometry (SIMS) U-Pb analyses made on the recrystallized titanite domains were interpreted to represent partial Pb-loss; neither yielded an impact age (McGregor et al., 2021).

5.2. Petrogenesis of titanite in Roter Kamm granite

In contrast to the examples from Sudbury, Vredefort, and Lac La Moinerie impact structures discussed above, the impact age of Roter Kamm (4 to 5 Ma) is very recent in comparison to the age of basement rocks and subsequent Proterozoic geologic history of the region. Age data combined with orientation analysis of Roter Kamm granite presented here unambiguously show that formation

of the granular titanite aggregates significantly pre-dated the Roter Kamm impact event. Granular microstructure in titanite from Roter Kamm granite exposed in the crater rim is thus an inherited product of regional Mesoproterozoic metamorphism, and is unrelated to the 4 to 5 Myr old crater-forming event.

A model is presented for formation of both titanite types in the Roter Kamm granite (Fig. 4). The crystallization age of the Roter Kamm granite (Fig. 4A) is well-established at 2020 ± 35 Ma, based on previously published U-Pb data from zircon grains in the same sample analyzed in this study (Thomas et al., 2016). The absence of *ca.* 2020 ages among 37 titanite grains analyzed here (Fig. 3) indicates that either all titanite grains were pervasively age-reset, or they all formed as secondary (metamorphic) phases after primary igneous crystallization.

A minor *ca.* 1875 Ma age component identified in some strained grains (Fig. 3A, D) represents the oldest ages detected in titanite from Roter Kamm granite. This age component is interpreted to record titanite formation during a Paleoproterozoic tectonothermal event that formed the foliation (Fig. 4B), and is likely related to deformation associated with intrusion of the voluminous 1910–1860 Ma Vioolsdrif magmatic suites (Thomas et al., 2016; Macey et al., 2017). Sample RT15-187 is peraluminous and is therefore unlikely to have crystallized primary amphibole or pyroxene; evidence of extensive plagioclase alteration, and the spatial association of titanite with abundant clinozoisite, epidote, and biotite (Supplementary Data Figs. S1, S2), are consistent with titanite and biotite forming by reaction(s) that involve ilmenite, clinozoisite (after plagioclase), alkali feldspar, and quartz (e.g., Harlov et al., 2006; Kohn, 2017) (Fig. 4B).

The prominence of *ca.* 1000–1050 Ma dates in all grains analyzed (Fig. 3) records a significant event which triggered some grains to recrystallize into neoblasts, and that reset U-Pb ages in nearly all titanite domains analyzed (Fig. 4C). The Mesoproterozoic ages are attributed to the terminal phase of the amphibolite-to-granulite facies *ca.* 1200–1000 Ma Namaqua Orogeny, which was associated with thermal metamorphism, major transcurrent shear zones, and coeval felsic magmatism (e.g. Thomas et al., 2016; Macey et al., 2018, Doggart, 2019). The absence of any post-Namaqua ages in the sample suite, especially recent Pb-loss (Fig. 3), precludes the neoblastic titanite textures from having formed during the 4 to 5 Ma Roter Kamm impact.

The timing of formation for observed crystal-plastic strain and $\{\bar{1}11\}$ deformation twins in titanite is less certain. Our model features formation of strained (Fig. 2A) and recrystallized titanite (Fig. 2B, C) in the context of a polyphase metamorphic history, involving tectonothermal events in the Paleoproterozoic (Fig. 4C), and later from 1200 to 1000 Ma (Fig. 4C). However, it is also possible that the strained grains and $\{\bar{1}11\}$ deformation twins (Fig. 4D) may record impact-related deformation. Timms et al. (2019) documented lamellar $\{\bar{1}11\}$ twins in titanite from granite in the Chicxulub peak ring, in a rock interpreted to record shock

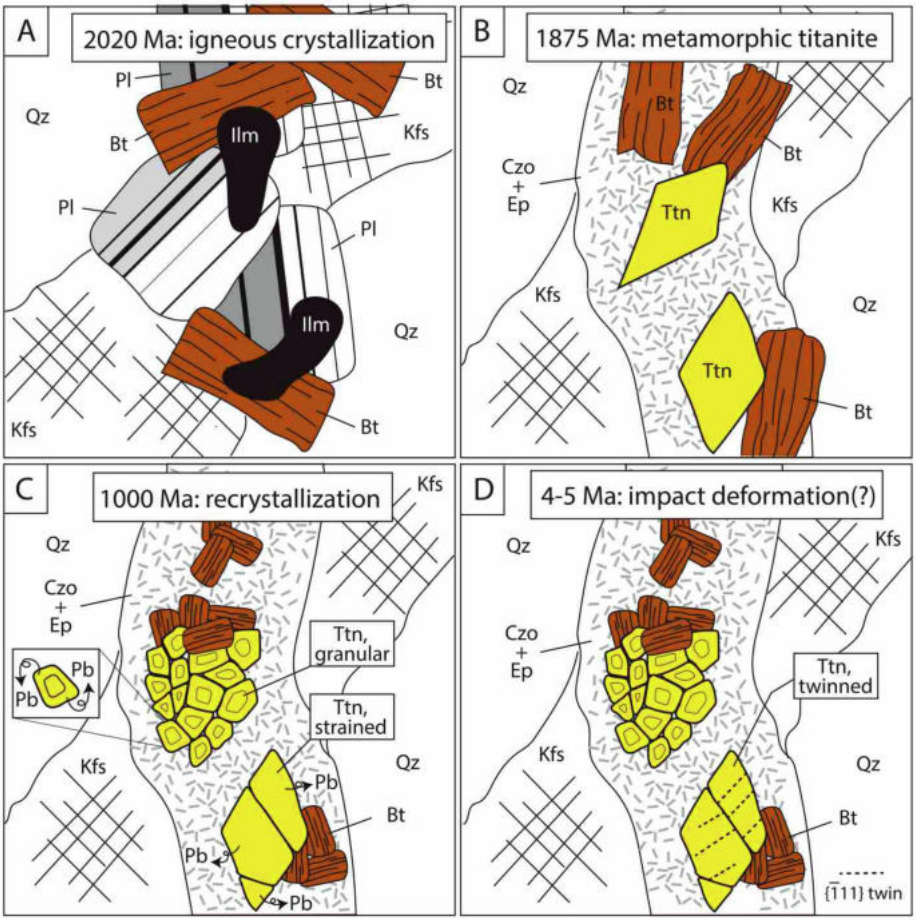

Fig. 4. Model for the evolution of titanite in Roter Kamm granite. (A) Igneous crystallization of Roter Kamm granite at *ca.* 2020 Ma; the presence of plagioclase (Pl) and ilmenite (Ilm) is inferred. (B) Formation of titanite (Ttn) and foliation during *ca.* 1875 Ma metamorphism. Plagioclase reacted to form epidote group minerals, along with ilmenite, to form titanite. (C) Static recrystallization of titanite and biotite (Bt), and localized deformation of non-neoblastic titanite at *ca.* 1000 Ma, along with near-complete age resetting of all titanite. (D) Formation of $\{\bar{1}11\}$ deformation twins in strained titanite during the 4–5 Myr Roter Kamm impact event, at pressure below 5 GPa (see text for discussion). Czo = clinozoisite; Ep = epidote; Kfs = alkali feldspar; Qz = quartz.

deformation at ~16–18 GPa based on microstructures in quartz (Feignon et al., 2020), and attributed {$\bar{1}$11} twin formation to shock deformation. The same {$\bar{1}$11} deformation twins in titanite from the Lac La Moinerie impact structure were also interpreted as having formed during shock deformation (McGregor et al., 2021). In this study, petrographic observation revealed no shock features in either quartz or biotite, and orientation mapping of 238 zircon grains from this sample also did not yield any evidence of impact-related deformation (Fig. A7) in the studied sample. If the {$\bar{1}$11} twins in Roter Kamm titanite are impact-related, they must have formed at conditions below which shock features form in quartz, which is generally thought to be <5 GPa (Stöffler and Langenhorst, 1994). Alternatively, the {$\bar{1}$11} twins may not be impact-related, and instead represent effects of Proterozoic deformation.

5.3. Origin of granular microstructure in titanite

Different deformation mechanisms can produce a granular microstructure in accessory minerals, and the combination of orientation analysis, age dating, and BSE imaging provide clues to its origin. Characteristic features that distinguish among formation process have been identified in studies of granular zircon (e.g., Piazolo et al., 2012), and are here considered for titanite. Studies of Sudbury granular titanite have cited dynamic recrystallization during shearing to explain highly elongate, foliation-parallel aggregates of neoblasts (Papapavlou et al., 2017). The nucleation of neoblastic titanite crystallites along twin boundaries has also been cited in different studies (e.g., Papapavlou et al., 2017; McGregor et al., 2021).

Roter Kamm neoblastic titanite differs from the above examples in that it does not have an apparent shape-preferred orientation (Fig. 2), nor is it localized along twin boundaries. There is also little evidence of fabric development during *ca.* 1000 Ma recrystallization, as biotite intergrown with neoblastic titanite is not aligned with, and does not define, a foliation (Fig. A2; Fig. 4C). Critical observations for the origin of granular titanite in Roter Kamm granite are the high-angle (>10°) grain boundaries among neoblasts (Figs. A5, A6), a lack of internal strain in individual neoblasts (<2°), straight grain boundaries that form triple junctions among generally equant neoblasts (Fig. 2B, C), ubiquitous oscillatory zoning in neoblasts, a lack of mineral alignment or elongation of aggregates, and the textural equilibrium with biotite (Fig. 2B, C). These observations are all consistent with a static, rather than dynamic, recrystallization process via heterogeneous nucleation and growth of new neoblast aggregates, which seemingly excludes processes such as fragmentation/rotation or subgrain rotation recrystallization (Piazolo et al., 2012). Equilibrium textures with biotite indicate an influx of fluid during recrystallization of titanite, which would further increase grain boundary mobility, and may have facilitated the formation of oscillatory zoning in titanite neoblasts (Fig. 3B, C).

Granular textured titanite was recently described from sheared gneiss in the Western Gneiss Region of Norway, a setting clearly unaffected by impact processes (Gordon et al., 2021). In this case, aggregates of strain-free titanite neoblasts form local triple junction grain boundaries and share high angle (>20°) grain boundaries with adjacent neoblasts. The Norway granular titanite was interpreted to represent the final product of prolonged tectonothermal deformation, involving crystal-plastic deformation (dislocation creep), dynamic and/or static recrystallization, grain boundary rotation, followed by annealing at amphibolite facies conditions (Gordon et al., 2021). Some aspects of the Norway granular titanite are similar to Roter Kamm granular titanite, such as the presence of triple junctions and high angle grain boundaries, but the absence of conspicuous features such as oscillatory zoning in the neoblasts suggests different formation processes.

We note that the application of U-Pb geochronology to extract impact ages from shock-deformed titanite is not limited to the study of recrystallized neoblastic grains. Timms et al. (2020) analyzed a microstructurally complex shock-twinned and hydrothermally altered titanite grain from a Chicxulub peak ring granitoid for U-Pb age by LAICPMS; a subset of the youngest ages determined were interpreted to have been age-reset during post-impact hydrothermal alteration, thus yielding an accurate impact age (e.g., Timms et al., 2020). McGregor et al. (2021) analyzed granular and non-granular titanite from impact melt at the Lac La Moinerie impact structure, but neither SIMS nor LAICPMS U-Pb data yielded an impact age. Our results highlight the need for careful consideration of granular titanite in rocks associated with impact events, as none of the examples described previously preserve both microstructures and ages that unambiguously correlate to the associated impact events. Such caution is particularly warranted when interpreting the origin of granular titanite in settings where the context is not known, such as granular grains in detrital suites (e.g., Cavosie et al., 2010, 2015; Montalvo et al., 2019) or in complex disaggregated rocks frequently found in impact settings, including breccia.

6. Conclusion

Our study of titanite grains from granite exposed in the rim of the Roter Kamm impact crater in Namibia combined EBSD orientation mapping and LAICPMS U-Pb geochronology to further investigate the origin of granular texture in titanite. Two populations of titanite were documented: strained grains, and strain-free neoblastic aggregates. The age data show that all titanite grains analyzed, including neoblastic domains, record Proterozoic tectonothermal events. No evidence of age resetting associated with the 4 to 5 Ma Roter Kamm impact was observed. Various aspects of the neoblastic titanite aggregates, including high angle grain boundaries, oscillatory zoning, lack of strain, and lack of shape preferred orientations, support their formation by static recrystallization processes. The origin of {1 1 1} deformation twins in strained titanite grains remains unclear, in terms of whether or not they represent evidence of shock deformation. Such twins have been reported previously in shock-deformed titanite grains from other impact structures, but typically in rocks that contain shocked quartz, which is absent in the Roter Kamm sample analyzed, thus indicating lower shock pressures. Further studies are needed to evaluate the formation conditions of {1 1 1} deformation twins in titanite to better understand their association with occurrences of granular textured titanite.

Declaration of Competing Interest

The authors declare that they have no known competing financial interests or personal relationships that could have appeared to influence the work reported in this paper.

Acknowledgements

Support was provided by the Space Science and Technology Centre at Curtin University, a Curtin Research Fellowship, and the Microscopy and Microanalysis Facility in the John de Laeter Centre at Curtin University. We thank Axel Wittmann and Max Webb for providing helpful reviews, and Nick Roberts for editorial handling. Laser ablation in the John de Laeter Centre is enabled by AuScope

(auscope.org.au) and the Australian Government via the National Collaborative Research Infrastructure Strategy (NCRIS).

Appendix A. Supplementary data

Supplementary data to this article can be found online at https://doi.org/10.1016/j.gsf.2022.101350.

References

Cavosie, A.J., Quintero, R.R., Radovan, H.A., Moser, D.E., 2010. A record of ancient cataclysm in modern sand: Shock microstructures in detrital minerals from the Vaal River, Vredefort Dome, South Africa. Geol. Soc. Am. Bull. 122 (11-12), 1968–1980. https://doi.org/10.1130/B30187.1.

Cavosie, A.J., Erickson, T.M., Timms, N.E., Reddy, S.M., Talavera, C., Montalvo, S.D., Pincus, M.R., Gibbon, R.J., Moser, D., 2015. A terrestrial perspective on using ex situ shocked zircons to date lunar impacts. Geology 43 (11), 999–1002. https://doi.org/10.1130/G37059.110.1130/2015335.

Cornell, D.H. Thomas, R.J. Gibson, R. Moen, H.F.G. Moore J.M., Reid D.L. 2006. Namaqua-Natal Province. In: Johnson, M.R., Anhauesser, C.R., Thomas, R.J. (Eds.), The Geology of South Africa. Geological Society of South Africa, Johannesburg/Council for Geoscience, Pretoria, 325-379.

Darling, J.R., Moser, D.E., Barker, I.R., Tait, K.T., Chamberlain, K.R., Schmitt, A.K., Hyde, B.C., 2016. Variable microstructural response of baddeleyite to shock metamorphism in young basaltic shergottite NWA 5298 and improved U-Pb dating of Solar System events. Earth Planet Sc. Lett. 444, 1–12.

Degenhardt Jr., J.J., Buchanan, P.C., Reid, A.M., Miller, R.M., 1994. Breccia veins and dykes associated with the Roter Kamm crater, Namibia. Geol. Soc. Am. Sp. Pap. 293, 197–208.

Doggart, S.W., 2019. Geochronology and isotopic characterisation of LCT pegmatites from the Orange River pegmatite province. Stellenbosch University, p. 234 pp.. M.S. thesis.

Erickson, T.M., Timms, N.E., Kirkland, C.L., Tohver, E., Cavosie, A.J., Pearce, M., Reddy, S.M., 2017. Shocked monazite chronometry: integrating microstructural and in situ isotopic age data for determining precise impact ages. Contrib. Mineral Petr. 172, 11.

Feignon, J.-G., FerriÈre, L., Leroux, H., Koeberl, C., 2020. Characterization of shocked quartz grains from Chicxulub peak ring granites and shock pressure estimates. Meteorit. Planet. Sci. 55 (10), 2206–2223.

Gordon, S.M., Kirkland, C.L., Reddy, S.M., Blatchford, H.J., Whitney, D.L., Teyssier, C., Evans, N.J., McDonald, B.J., 2021. Deformation-enhanced recrystallization of titanite drives decoupling between U-Pb and trace elements. Earth Planet. Sci. Let. 560, 116810. https://doi.org/10.1016/j.epsl.2021.116810.

Grieve, R., Therriault, A., 2000. Vredefort, Sudbury, Chicxulub: Three of a kind? Annu. Rev. Earth Planet. Sci. 28 (1), 305–338.

Hauser, N., Reimold, W.U., Cavosie, A.J., Crosta, A.P., Schwarz, W.H., Trieloff, M., Maia, D.S., de Souzai, C., Pereira, L.A., Rodriguesi, E.N., Brown, M., 2019. Linking shock textures revealed by BSE, CL, and EBSD with U-Pb data (LA-ICPMS and SIMS) from zircon from the Araguainha impact structure, Brazil. Meteorit. Planet. Sci. 54, 2286–2311.

Harlov, D., Tropper, P., Seifert, W., Nijland, T., Förster, H.-J., 2006. Formation of Al-rich titanite ($CaTiSiO_4O$-$CaAlSiO_4OH$) reaction rims on ilmenite in metamorphic rocks as a function of fH_2O and fO_2. Lithos 88, 72–84.

Hecht, L., Reimold, W.U., Sherlock, S., Tagle, R., Koeberl, C., Schmitt, R.-T., 2008. New impact-melt rock from the Roter Kamm impact structure, Namibia: Further constraints on impact age, melt rock chemistry, and projectile composition. Meteorit. Planet. Sci. 43 (7), 1201–1218.

Kenny, G.G., Morales, L.F., Whitehouse, M.J., Petrus, J.A., Kamber, B.S., 2017. The formation of large neoblasts in shocked zircon and their utility in dating impacts. Geology 45 (11), 1003–1006.

Kenny, G.G., Schmieder, M., Whitehouse, M.J., Nemchin, A.A., Morales, L.F.G., Buchner, E., Bellucci, J.J., Snape, J.F., 2019. A new U-Pb age for shock-recrystallised zircon from the Lappajärvi impact crater, Finland, and implications for the accurate dating of impact events. Geochim. Cosmochim. Acta 245, 479-494.

Kenny, G.G., Karlsson, A., Schmieder, M., Whitehouse, M.J., Nemchin, A.A., Bellucci, J. J., 2020. Recrystallization and chemical changes in apatite in response to hypervelocity impact. Geology 48 (1), 19–23.

Koeberl, C., Hartung, J.B., Kunk, M.J., Klein, J., Matsuda, J.-I., Nagao, K., Reimold, W.U., Storzer, D., 1993. The age of the Roter Kamm impact crater, Namibia: Constraints from ^{40}Ar-^{39}Ar, K-Ar, Rb-Sr, fission track, and ^{10}Be-^{26}Al studies. Meteoritics 28 (2), 204–212.

Kohn, M.J., 2017. Titanite petrochronology. Rev. Mineral. Geochem. 83, 419–441.

Krogh, T.E., Davis, D.W., Corfu, F., 1984. Precise U-Pb zircon and baddeleyite ages for the Sudbury area. In: Pye, E.G., et al., (Eds.), The Geology and Ore Deposits of the Sudbury Structure. Ontario Geol. Surv. Special Volume 1, 431–446.

Macey, P.H., Thomas, R.J., Minnaar, H.M., Gresse, P.G., Lambert, C.W., Groenewald, C., Miller, J.A., Indongo, J., Angombe, M., Shifotoka, G., Frei, D., Diener, J.F.A., Dhansay, T., Kisters, A.F.M., le Roux, P., Smith, H., 2017. The Palaeoproterozoic Richtersveld Magmatic Arc: remnant root of the Mesoproterozoic Namaqua Orogen, SW Africa. Precambrian Res. 292, 417–451. https://doi.org/10.1016/j.precamres.2017.01.013.

Macey, P.H., Bailie, R.H., Miller, J.A., Thomas, R.J., de Beer, C., Frei, D., le Roux, P.J., 2018. Implications of the distribution, age and origins of the granites of the Mesoproterozoic Spektakel Suite for the timing of the Namaqua Orogeny in the Bushmanland Subprovince of the Namaqua-Natal Metamorphic Province. South Africa. Precambrian Res. 312, 68–98.

McGregor, M., Dence, M.R., McFarlane, C.R.M., Spray, J.G., 2020. U-Pb geochronology of apatite and zircon from the Brent impact structure, Canada: a Late Ordovician Sandbian-Katian boundary event associated with L-Chondrite parent body disruption. Contrib. Mineral. Petr. 175, 63. https://doi.org/10.1007/s00410-020-01699-9.

McGregor, M., Erickson, T.M., Spray, J.G., Whitehouse, M.J., 2021. High-resolution EBSD and SIMS U-Pb geochronology of zircon, titanite, and apatite: insights from the Lac La Moinerie impact structure, Canada. Contrib. Mineral. Petr. 176, 76. In press.

Montalvo, P.E., Cavosie, A.J., Kirkland, C.L., Evans, N.J., McDonald, B.J., Talavera, C., Erickson, T.M., Lugo-Centeno, C., 2019. Detrital shocked zircon provides first radiometric age constraint (<1472 Ma) for the Santa Fe impact structure, New Mexico, USA. Geol. Soc. Am. Bull. 131, 845–863.

Piazolo, S., Austrheim, H., Whitehouse, M., 2012. Brittle-ductile microfabrics in naturally deformed zircon: Deformation microstructures and consequences for U-Pb dating. Am. Mineral. 97, 1544–1563.

Papapavlou, K., Darling, J.R., Storey, C.D., Lightfoot, P.C., Moser, D.E., Lasalle, S., 2017. Dating shear zones with plastically deformed titanite: New insights into the orogenic evolution of the Sudbury impact structure (Ontario, Canada). Precambrian Res. 291, 220–235.

Papapavlou, K., Darling, J.R., Moser, D.E., Barker, I.R., EIMF, White, L.F., Lightfoot, P.C., Storey, C.D., Dunlop, J., 2018. U-Pb isotopic dating of titanite microstructures: potential implications for the chronology and identification of large impact structures. Contrib. Mineral. Petr. 173, 82.

Rajmon, D., Copeland, P., Reid, A.M., 2005. Argon isotopic analysis of breccia veins from the Roter Kamm crater, Namibia, and implications for their thermal history. Meteor. Planet. Sci. 40, 841–854.

Rasmussen, C., Stockli, D.F., Erickson, T.M., Schmieder, M., 2020. Spatial U-Pb age distribution in shock-recrystallized zircon –A case study from the Rochechouart impact structure, France. Geochim. Cosmochim. Acta 273, 313–330.

Reimold, W.U., Miller, R.M., 1989. The Roter Kamm impact crater, SWA/Namibia. In: Proceedings of the 19th Lunar Planet. Sci. Conf, pp. 711–732.

Reimold, W.U., Koeberl, C., Bishop, J., 1994. Roter Kamm impact crater, Namibia: Geochemistry of basement rocks and breccias. Geochim. Cosmochim. Acta 58, 2689–2710.

Reimold, W.U., Koeberl, C., Brandt, D., 1997. Suevite at Roter Kamm impact crater, Namibia. Meteoriti. Planet. Sci. 32, 431–437.

Schlüter, T., 2008. Geological atlas of Africa: with notes on stratigraphy, tectonics, geosites and geoscientific education of each country. Springer-Verlag, Berlin, Heidelberg, New York, 307 pp. doi:10.1017/S0016756809006281

Stöffler, D., Langenhorst, F., 1994. Shock metamorphism of quartz in nature and experiment: I. Basic observation and theory. Meteoriti. Planet. Sci. 29, 155–181.

Thomas, R.J., Macey, P.H., Spencer, C., Dhansay, T., Diener, J.F.A., Lambert, C.W., Frei, D., Nguno, A., 2016. The Sperrgebiet Domain, Aurus Mountains, SW Namibia: A ~2020–850 Ma window within the Pan-African Gariep Orogen. Precambrian Res. 286, 35–58.

Timms, N.E., Kirkland, C.L., Cavosie, A.J., Rae, A.S.P., Rickard, W.D.A., Evans, N.J., Erickson, T.M., Wittmann, A., Ferrière, L., Collins, G.S., Gulick, S.P.S., 2020. Shocked titantite records Chicxulub hydrothermal alteration and impact age. Geochim. Cosmochim. Acta 281, 12–30.

Timms, N.E., Pearce, M.A., Erickson, T.M., Cavosie, A.J., Rae, A., S.P., Wheeler, J., Wittmann, A., Ferrière, L., Poelchau, M.H., Tomioka, N., Collins, G.S., Gulick, S.P. S., Rasmussen, C., Morgan, J.V., 2019. New shock microstructures in titanite ($CaTiSiO_5$) from the peak ring of the Chicxulub impact structure, Mexico. Contrib. Mineral. Petr. 174, 38.